Homogeneous Catalysis

Lewis Acids as Activators in CBS-Catalysed Diels–Alder Reactions: Distortion Induced Lewis Acidity Enhancement of $SnCl_4$

Alexander R. Nödling, Robert Möckel, Ralf Tonner,* and Gerhard Hilt*[a]

Dedicated to Prof. Dr. Gernot Frenking on the occasion of his 70th birthday

Abstract: The effect of several Lewis acids on the CBS catalyst (named after Corey, Bakshi and Shibata) was investigated in this study. While ^{2}H NMR spectroscopic measurements served as gauge for the activation capability of the Lewis acids, in situ FT-IR spectroscopy was employed to assess the catalytic activity of the Lewis acid oxazaborolidine complexes. A correlation was found between the $\Delta\delta(^2H)$ values and rate constants k_{DA}, which indicates a direct translation of Lewis acidity into reactivity of the Lewis acid–CBS complexes. Unexpectedly, a significant deviation was found for $SnCl_4$ as Lewis acid. The $SnCl_4$–CBS adduct was much more reactive than the $\Delta\delta(^2H)$ values predicted and gave similar reaction rates to those observed for the prominent $AlBr_3$–CBS adduct. To rationalize these results, quantum mechanical calculations were performed. The frontier molecular orbital approach was applied and a good correlation between the LUMO energies of the Lewis acid–CBS–naphthoquinone adducts and k_{DA} could be found. For the $SnCl_4$–CBS–naphthoquinone adduct an unusual distortion was observed leading to an enhanced Lewis acidity. Energy decomposition analysis with natural orbitals for chemical valence (EDA-NOCV) calculations revealed the relevant interactions and activation mode of $SnCl_4$ as Lewis acid in Diels–Alder reactions.

Introduction

Chiral oxazaborolidines were introduced by Itsuno as reagents,[1] and refined by Corey for catalytic use in asymmetric reductions of prochiral ketones with boranes nearly 30 years ago.[2] Due to their widespread use as powerful and versatile catalysts,[3] (*S*)-proline-derived oxazaborolidines **1** are usually referred to as CBS catalysts, stemming from the initials of the authors Corey, Bakshi, and Shibata in their seminal report (Figure 1).[2]

In the last decade, the Corey group could expand the reaction scope of oxazaborolidine catalysts **1** by combining them with superacids such as TfOH or Tf_2NH.[4] This results in protonation of the nitrogen atom of **1**, thus enhancing the Lewis acidity of the adjacent boron atom. These protonated species of type **3** (Scheme 1) are potent catalysts in asymmetric Diels–Alder reactions of α,β-unsaturated carbonyl compounds.[5] Shortly after, (*S*)-valine-derived oxazaborolidine (**2**) was developed by Yamamoto.[6] The combination of Lewis acids (LA), for example, $SnCl_4$, $TiCl_4$ or $FeCl_3$, with **2** led to a similar Lewis acidity enhancement of the boron atom by coordination of the Lewis acid to the nitrogen. In this case, the Lewis acids showed superior reactivities and enantioselectivities in Diels–Alder reactions than the superacids TfOH or Tf_2NH. Corey subsequently found $AlBr_3$ as a highly potent activator of **1 b** for Diels–Alder reactions,[7] but mentioned worse results when other Lewis acids, such as BCl_3 or $SnCl_4$, were used.[8] Both catalysts, **1 a/b** and **2**, have found regular use, for example, in natural product synthesis, but mainly as their protonated congeners **3 a/b**.[5,9] Reports on the use of Lewis acid-activated oxazaborolidines, such as **4**, are scarce,[9g,10] and if Lewis acids are used, $AlBr_3$ is employed almost exclusively.

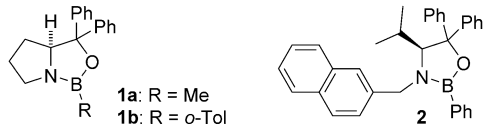

Figure 1. Chiral oxazaborolidines **1 a**, **1 b** and **2** as introduced by Corey and Yamamoto.

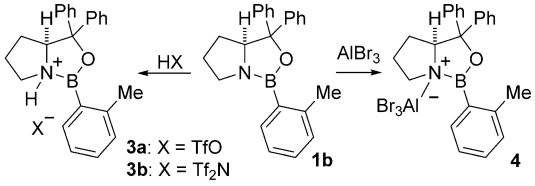

Scheme 1. Activation of oxazaborolidine **1 b** by Brønsted or Lewis acid.

[a] Dr. A. R. Nödling, R. Möckel, Dr. R. Tonner, Prof. Dr. G. Hilt
Fachbereich Chemie, Philipps-Universität Marburg
Hans-Meerwein-Straße 4, 35032 Marburg (Germany)
E-mail: Tonner@chemie.uni-marburg.de
Hilt@chemie.uni-marburg.de

Supporting information for this article is available on the WWW under http://dx.doi.org/10.1002/chem.201602394.

Due to our interest in the relation between experimentally quantifiable strength and catalytic activity of Lewis acids,[11] we were curious about the underlying reasons for the apparent superiority of $AlBr_3$ as activator of **1 b** compared to other Lewis acids. We envisaged the polarising effect on the oxazaborolidine framework upon Lewis acid coordination to be experimentally quantifiable by an ^{2}H NMR spectroscopic probe. Based on our previous experience of quantifying the Lewis acidity of metal(loid) halides with quinolizidine probe [D$_1$]**5**,[11a] we expected to be able to quantify the activation of **1 b** upon coordination of a Lewis acid via ^{2}H NMR spectroscopic studies of the deuterated derivative [D$_1$]**1 b** (Figure 2).

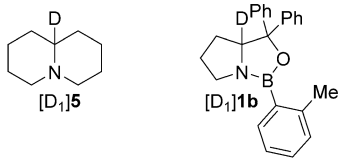

Figure 2. ^{2}H NMR spectroscopical probes quinolizidine [D$_1$]**5** and the deuterated CBS catalyst [D$_1$]**1 b**.

The shift difference $\Delta\delta(^2H)$ between the ^{2}H NMR shift of the respective Lewis acid–oxazaborolidine complex and the free oxazaborolidine [D$_1$]**1 b** would serve as quantified activation of [D$_1$]**1 b**. As encountered in our previous studies,[11a] we anticipated the activation $\Delta\delta(^2H)$ of [D$_1$]**1 b** in Lewis acid complexes to correlate with catalytic activity of such complexes in organic transformations, such as the Diels–Alder reaction (DA). To probe this relation we intended to conduct kinetic studies of a representative Diels–Alder reaction using in situ FT-IR spectroscopy. Thereby, rate constants, k_{DA}, should be obtained for different Lewis acid–CBS complexes and in addition enantiomeric ratios should be determined for probing the performance of different Lewis acids.

Results and Discussion

Synthesis of deuterated oxazaborolidine probe [D$_1$]1 b

The deuterated oxazaborolidine [D$_1$]**1 b** was synthesised by combining a modified procedure of Gilmour for the synthesis of deuterated amino alcohol [D$_1$]**8** and the condensation protocol reported by Yamamoto (Scheme 2).[12,13] The deuterium content was determined by ^{1}H NMR spectroscopy after Grignard addition of PhMgBr to deuterated ester [D$_1$]**7**, and was on average about 80%. The deuterated oxazaborolidine [D$_1$]**1 b** could be obtained after condensation of [D$_1$]**8** with tri-*ortho*-tolylboroxine in acceptable yield and with sufficient deuterium content.

^{2}H NMR spectroscopic studies of Lewis acid–CBS complexes of type 6

We chose a number of common Lewis acids for the study, ranging from $BF_3{\cdot}Et_2O$ to very strong $AlBr_3$ and included the

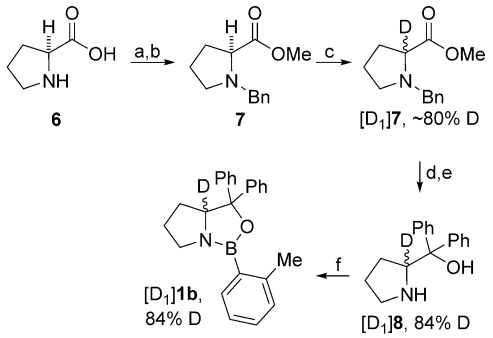

Scheme 2. Synthesis of deuterated oxazaborolidine [D$_1$]**1 b**. a) $SOCl_2$, MeOH, 0 °C to RT, 16 h; b) toluene/NEt_3 1:1, BnBr, reflux, 16 h, quantitative yield over 2 steps; c) LDA, THF, −20 °C, 1 h, then D_2O, −5 °C to RT, 16 h, 78%; d) PhMgBr, THF, 5 °C to RT, 16 h, 64%, 84% D; e) Pd/C (10% Pd), HCl, H_2 (1 atm), EtOH, quantitative yield; f) tri-*ortho*-tolylboroxine, toluene, reflux, Dean–Stark apparatus, quantitative yield. Bn = benzyl, Ph = phenyl, LDA = lithium diisopropylamide. For details see the Supporting Information.

frequently used Brønsted acid $HNTf_2$ (Table 1). In order to assess the activation the chemical shift $\Delta\delta(^2H)$ of [D$_1$]**1 b** upon Lewis acid coordination was measured. Therefore, we applied the procedure which we developed for quinolizidine probe [D$_1$]**5**.[11a] Therein, [D$_1$]**5** is treated with a tenfold excess of Lewis acid in CH_2Cl_2 at room temperature. In case of [D$_1$]**1 b** this excess was diminished to five equivalents of Lewis acids, since in the case of insoluble Lewis acids that form soluble complexes, for example, $AlCl_3$ or InI_3, a better signal-to-noise ratio was observed. ^{2}H NMR spectroscopic titration experiments of [D$_1$]**1 b** with InI_3 showed a single, downfield shifted peak throughout the titration, and minimal difference of $\Delta\delta(^2H)$ at five or ten equivalents of InI_3. Therefore, we embarked on further studies including all acids under these conditions (Table 1).

The ^{2}H NMR spectroscopic studies using excess Lewis acid revealed several interesting aspects. The activation $\Delta\delta(^2H)$ is connected to the quantified or the perceived acidity of Lewis acids, for example, $BF_3{\cdot}Et_2O$ activates [D$_1$]**1 b** less than $AlCl_3$ or BBr_3.[14] Furthermore, some Lewis acids displayed none or hardly any activation, for example, ZnI_2 or $InCl_3$. Finally, some Lewis acid–CBS adducts exhibited several signals in the respective ^{2}H NMR spectra, hence more than one species must be formed.[15]

The rationale for more than one peak in ^{2}H NMR spectra could be traced back to coordination of the Lewis acid to the oxygen atom of [D$_1$]**1 b**,[16] as well as via adducts with simultaneous coordination of two Lewis acid molecules to the nitrogen and the oxygen atom of [D$_1$]**1 b**. The latter could be responsible for the very high $\Delta\delta(^2H)$ values observed in some cases, for example, for $AlBr_3$ or $TiCl_4$ (see the Supporting Information for quantum chemical calculations on the stability of N–, O–, and N–O-coordinated adducts **9**; Table S2). We additionally suspected decomposition of adducts **9** since no clear precedence was present, as Corey mentioned a stability of **9 e** only below −20 °C,[5] whereas Paddon-Row used the $SnCl_4$

Table 1. ^{2}H NMR spectroscopic quantified activation $\Delta\delta(^2H)$ of [D$_1$]**1b** upon Lewis acid coordination at −40 °C.

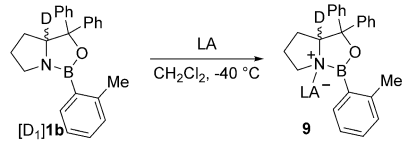

$\delta(^2H)$ = 4.54 ppm $\delta(^2H)$ > 4.54 ppm

Entry[a]	Lewis acid	CBS adduct	$\Delta\delta(^2H)$ [ppm] (−40 °C)
1	$BF_3{\cdot}Et_2O$	**9a**	0.00
2	BCl_3	**9b**	**1.14**, 0.28[d]
3	BBr_3	**9c**	1.20
4	$AlCl_3$	**9d**	**1.22**, 0.29[d]
5	$AlBr_3$	**9e**	1.27[b]
6	AlI_3	**9f**	1.28[c]
7	$InCl_3$	**9g**	0.00
8	$InBr_3$	**9h**	0.00
9	InI_3	**9i**	0.81
10	$SnCl_4$	**9j**	0.16
11	$TiCl_4$	**9k**	0.49
12	ZnI_2	**9l**	–
13	$HNTf_2$	**3b**	**0.83**, 0.46, 0.22[d]

[a] Adducts **3b** and **9** were prepared according to the general procedure 1 (see the Supporting Information): [D$_1$]**1b** (64 µmol, 1.0 equiv), Lewis acid (64 µmol, 1.0 equiv), CH_2Cl_2 (0.50 mL), preparation below −70 °C, NMR spectroscopic measurement was then performed at −40 °C. [b] CH_2Br_2 was used as solvent instead of CH_2Cl_2. [c] CH_2I_2 was used as solvent instead of CH_2Cl_2. [d] The most intensive peak is given in bold format.

adduct **9j** at 40 °C.[17] We found the $AlCl_3$ adduct **9d** to decompose at room temperature over the course of 24 h.

To circumvent these problems the 1:1 adducts (ratio of Lewis acid/[D$_1$]**1b**) were synthesised below −70 °C and investigated by ^{2}H NMR spectroscopy at three different temperatures. As expected, the number of signals was reduced at low temperatures whereas at room temperature several species were observable (for the complete data set at different temperatures, see the Supporting Information, Table S1).

No $\Delta\delta(^2H)$ value could be obtained for $BF_3{\cdot}Et_2O$, since a precipitate formed at −70 °C, which we assume to be either solid $BF_3{\cdot}Et_2O$ (m.p. about −58 °C) or **9a**. The most consistent data set of $\Delta\delta(^2H)$ values was found at −40 °C (Table 1) and is used for further discussion (25 °C in case of $BF_3{\cdot}Et_2O$). In case of the 1:1 adducts a clearer connection between Lewis acidity and activation of [D$_1$]**1b** was notable, that is, an increase of $\Delta\delta(^2H)$ values for a given central atom with heavier halide substituents, for example, Table 1, entries 1–3. In addition, it became clear that several Lewis acids, for example, BCl_3, BBr_3, or $AlCl_3$, exerted a similar polarising effect on [D$_1$]**1b** as $AlBr_3$.

Considering all employed acids, four groups of activators could be distinguished based on the $\Delta\delta(^2H)$ values (Figure 3). This classification matches to a good degree with the acidities of these Lewis acids as determined by other experimental quantification methods.[14] Accordingly, we assumed that the adducts **9** formed with these Lewis acids should be equally good catalysts in Diels–Alder reactions, if the catalytic activity would correlate strictly to the activation of **1b**.

strong activation	moderate activation
$\Delta\delta(^2H)$ > 1.00 ppm **BCl_3, BBr_3** **$AlCl_3$, $AlBr_3$** **AlI_3**	0.50 ppm < $\Delta\delta(^2H)$ < 1.00 ppm **InI_3** **$HNTf_2$**
weak activation	**no activation**
0.00 ppm < $\Delta\delta(^2H)$ < 0.50 ppm **$SnCl_4$** **$TiCl_4$** **$BF_3{\cdot}Et_2O$ (at 25 °C)**	$\Delta\delta(^2H) \cong$ 0.00 ppm **ZnI_2** **$InCl_3$** **$InBr_3$**

Figure 3. Classification of the investigated Lewis acids depending on their activation of [D$_1$]**1b**.

In situ FT-IR spectroscopic kinetic studies of Diels–Alder reactions catalysed by Lewis acid-CBS complexes 9

The transformation has the advantage that the progress of the reaction can easily be monitored by in situ FT-IR spectroscopy. Another aspect was that the enantioselectivity was not excellent when the $AlBr_3$–CBS catalyst was used which leaves room to track the influence of other Lewis acids.[7]

The Diels–Alder reactions were performed under pseudo-first-order conditions regarding **10** with a tenfold excess of isoprene (**11**) and by using 4.0 mol% of active catalyst adduct **3b** or **9** (Scheme 3). In contrast to Corey's procedure, the Lewis acid–CBS adducts **3b** and **9** were prepared in a separate flask and added to the reactant mixture, since in some cases, for example, BBr_3, a precipitate was observed, if Lewis acid–CBS catalysts were mixed with **10** before **11** was added. A slight excess of oxazaborolidine **1b** with respect to the Lewis acid was used to avoid racemic background reaction.

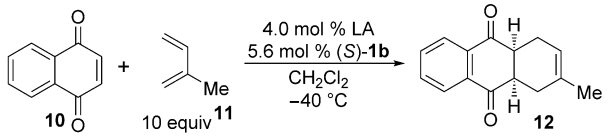

Scheme 3. Diels–Alder reaction to determine rate constants for different Lewis acids (LA).

The reaction progress was monitored by following the carbonyl bands of **10** and **12**, at 1670 and 1696 cm^{-1}, respectively. The changes in concentrations were then used to calculate the rate constants k_{DA}. A comparison of all measured concentration profiles for adducts **9** is given in Figure 4, and an overview of the kinetic data (averages of at least three measurements) is given in Table 2.

The profiles, excluding the one obtained with BF_3 adduct **9a**, showed a bend after 150 to 250 seconds, which we so far attribute to experimental constraints. Before and after the bend straight fits were observed, as expected for a reaction under pseudo-first-order conditions. Therefore, we calculated the constants before, $k_{DAStart}$ (see the Supporting Information), and after the bend k_{DA} (Table 2). In case of full conversion the

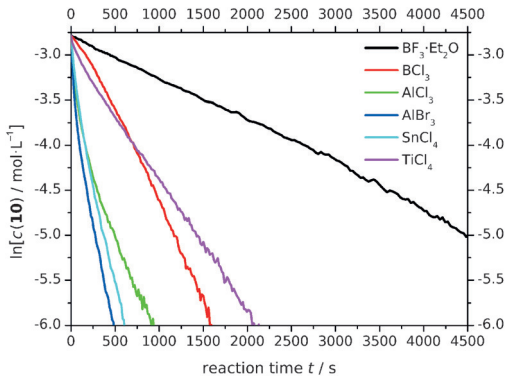

Figure 4. Plots of the natural logarithms of the concentration profiles versus the reaction time obtained with Lewis acid–CBS adducts **9a**, **9b**, **9d**, **9e**, **9j**, and **9k** as catalysts in the Diels–Alder reaction between **10** and **11**.

Table 2. Kinetic data and enantioselectivities of Diels–Alder reactions between **10** and **11** catalysed by CBS adducts **3b** and **9**.

Entry[a]	LA/adduct	$k_{DA}\times10^{-4}$ [s^{-1}][a]	e.r.
1	$BF_3{\cdot}Et_2O$/**9a**	4.2 ± 0.8	69:31
2	BCl_3/**9b**	23.7 ± 1.9	55:45
3	BBr_3/**9c**	–[b]	90:10
4	$AlCl_3$/**9d**	34.5 ± 20.5	86:14
5	$AlBr_3$/**9e**	43.0 ± 10.5	83:17
6	AlI_3/**9f**	–[c]	81:19
7	$InCl_3$/**9g**	–[c]	–
8	$InBr_3$/**9h**	–[c]	–
9	InI_3/**9i**	–[c]	89:11
10	$SnCl_4$/**9j**	45.6 ± 8.8	93:7
11	$TiCl_4$/**9k**	14.0 ± 4.2	89:11
12	ZnI_2/**9l**	–[c]	–
13	$HNTf_2$/**3b**	–[c]	–

[a] Reaction conditions according to the general procedure 3 (see the Supporting Information): 1,4-naphthoquinone (**10**, 0.50 mmol, 1.0 equiv), isoprene (**11**, 5.00 mmol, 10.0 equiv), **1b** (28 µmol, 5.6 mol%), Lewis acid (20 µmol, 4.0 mol%), CH_2Cl_2 (7.6 mL), −40 °C, see the Supporting Information for details. The given value is the mean of three reactions. [b] Reactions with BBr_3 were irreproducible, hence no k_{DA} is given. [c] The conversion was below 10% after 8 h reaction time.

reaction was quenched followed by a short work-up to determine the enantiomeric ratios by chiral LC analysis (Table 2). The kinetic measurements showed several surprising features. First of all, some adducts exhibited none or a very small catalytic activity in the monitored timeframe of up to ten hours, namely the adducts of **1b** with AlI_3, all indium halides, ZnI_2, BBr_3 and $HNTf_2$. This was not surprising for $InCl_3$ and $InBr_3$, since they do not activate **1b** according to the $\Delta\delta(^2H)$ values. Adduct **3b** was employed by Corey in similar reactions and usually 20 mol% of **3b** are used or reaction times of at least 12 h are necessary. So despite its moderate activation of **1b**, which is still higher than that of catalytically highly active adducts, for example, **9j**, the formation of contact ion pairs in **3b** seems to prevent a higher activity and measurable rates under the reaction conditions employed in this study.[4a]

While InI_3 adduct **9i** was found to be active at room temperature in preliminary studies, the Diels–Alder reaction with AlI_3 adduct **9f** did not reach full conversion even after 12 h at room temperature. The interpretation of the kinetic data for the activation with the BBr_3–CBS adduct **9c** was hampered based on competing oligomerisation of the isoprene. For the visualisation of a correlation the Lewis acidity strength, determined by the $\Delta\delta(^2H)$ values, and the catalytic activities, namely, the rate constants k_{DA}, were plotted (Figure 5; a plot of $k_{DAStart}$ vs. $\Delta\delta(^2H)$ is given in the Supporting Information, Figure S3).

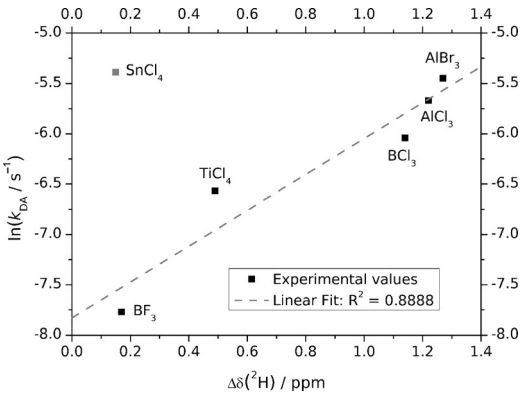

Figure 5. Plot of the natural logarithms of k_{DA} values versus the $\Delta\delta(^2H)$ values. The linear fit was obtained with exclusion of $SnCl_4$ adduct **9j**.

First, with exclusion of $SnCl_4$ adduct **9j** a moderate correlation is observed. The activity of adducts **9** and activation of **1b** is in agreement with the usually perceived and experimentally quantified acidity of the respective Lewis acids,[11a,14] that is, $AlBr_3$ activates **1b** more and adduct **9e** is more active than $TiCl_4$ and its adduct **9k**. Second, an unexpected discrepancy is observed for $SnCl_4$ adduct **9j**, which catalysed the Diels–Alder reaction between **10** and **11** much faster than the $\Delta\delta(^2H)$ suggested. This runaway value prompted the quantum chemical investigations shown in the next subsection.

Overall, the NMR spectroscopic chemical shifts $\Delta\delta(^2H)$ correlated well with the rate constants which are in agreement to Corey's observations as well as to Fujimoto's theoretical studies.[16] Generally, a higher Lewis acidity of a given Lewis acid leads to a stronger activation of **1b**, which was measurable by ^2H NMR spectroscopy employing [D_1]**1b**, and a higher catalytic activity of Lewis acid–CBS adducts **9**. The $AlBr_3$ adduct **9e** shows the highest activation, and with the $SnCl_4$ adduct **9j** the highest activities as catalysts in Diels–Alder reactions.[18]

Despite the low activities or side reactions observed with adducts **9c**, **9f**, and **9i** the enantioselectivities were decent (**9f**) to good (**9c**, **9i**) and even better for the $SnCl_4$–CBS adduct (**9j**) reaching the highest e.r. of 93:7. Concerning the enantioselectivities of active adducts **9** nearly no enantioselectivity was found for **9a** and **9b**. Good enantioselectivities were observed for **9i**, **9j** and **9k**, while the $AlBr_3$ adduct **9e** yielded a lower e.r. value than reported by Corey.[7] This could be attributed to the higher reaction temperature applied in this study, or the fact that $AlBr_3$ was used in substance instead of a commercially available 1.0 M solution.

Quantum chemical calculations: frontier molecular orbitals

The surprising findings for InI_3 (no catalytic activity despite significant $\Delta\delta(^2H)$ value) and $SnCl_4$ (very high catalytic activity despite moderate $\Delta\delta(^2H)$ value) prompted computational investigation of the Lewis acid interactions with the CBS catalyst. We used density functional theory approaches with two different functionals for structural optimisation (M06-2X/def-2TZVP) and bonding analysis (BP86/TZ2P$^+$).

Frontier molecular orbital (FMO) theory is a common approach to estimate the reactivity change of a dienophile upon Lewis acid coordination and can be expressed as LUMO lowering $\Delta E_{LUMO} = E_{LUMO(\mathbf{10}\text{–CBS–LA})} - E_{LUMO(\mathbf{10})}$.[19] A correlation between ΔE_{LUMO} and rate constants has been elucidated by Laszlo for simple aluminium halides several decades ago in a rather unnoticed account.[20] The appeal of FMO theory is its simplicity and its applicability to reactants instead of a tedious transition state analysis.

Based on these studies we started our approach by optimising the structures of the complexes formed from 1,4-naphthoquinone (**10**) and Lewis acid–CBS adducts **9** (in the following referred to as **10**–Lewis acid–CBS complexes **13**) in order to check whether it is possible to use ΔE_{LUMO} to predict the reactivity of 1,4-naphthoquinone (**10**). A preliminary justification for this approach is given in Figure 6, showing the LUMO of **13j**, which is completely localised on the 1,4-naphthoquinone moiety. Subsequently, the energy differences ΔE_{LUMO} were calculated for all Lewis acids applied in the spectroscopic and kinetic studies (these are summarised in the Supporting Information, Table S2). To verify the predictive power of ΔE_{LUMO} for the catalytic activity of adducts **9** in the Diels–Alder reaction of **10** with **11** ΔE_{LUMO} was plotted against the measured rate constants k_{DA}. The results for adducts **9** that showed significant rate constants are presented in Figure 7. In contrast to the plot of $\Delta\delta(^2H)$ versus $\ln(k_{DA})$ (Figure 5), there is a much better correlation between ΔE_{LUMO} and $\ln(k_{DA})$ for all catalytically active adducts **9** obtained with $AlCl_3$, $AlBr_3$, $TiCl_4$, BF_3, BCl_3, and especially with $SnCl_4$. Furthermore, the Lewis acids with no significant k_{DA} showed low ΔE_{LUMO} as well, demonstrating the predictive power of the FMO approach.

In case of the indium-based Lewis acids, a rather simple explanation for the low reactivity could be found. Although all indium Lewis acids coordinate quite well to CBS catalyst **1b** (see the Supporting Information, Table S3), and therefore show a significant NMR shift $\Delta\delta(^2H)$, 1,4-naphthoquinone (**10**) does not coordinate to the boron atom in complexes **13g–i**, but to the indium atom (Tables S5 and S6).[21] Thereby, the activation of **10** is only mediocre and CBS adducts **9g–i** exhibit only very small catalytic activity as catalyst in Diels–Alder reactions.

As we were able to explain the low activity of the indium Lewis acid–CBS adducts **9g–i**, we turned our attention to the strange behaviour of $SnCl_4$–CBS adduct **9j**. The low activation of **1b** but very good activation of **10** by $SnCl_4$-based adduct **9j** in the model Diels–Alder reaction is confusing at first sight. In most studies, $SnCl_4$ is usually regarded as a weak to moderate strong Lewis acid and thus the low activation $\Delta\delta(^2H)$ of **1b** is in line with existing evidence.[11a,14] Hence, the notwithstanding

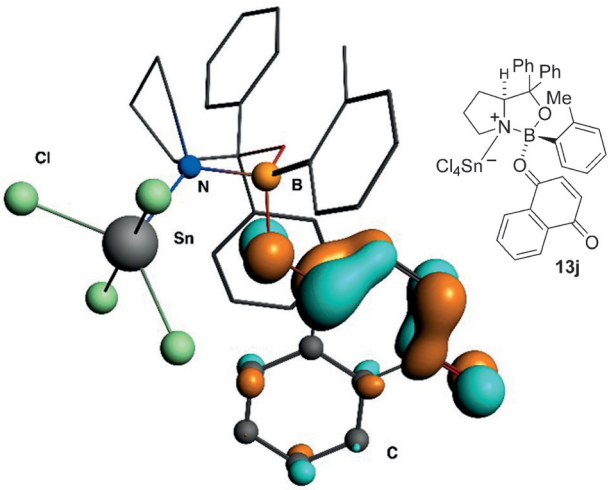

Figure 6. Plot of the calculated LUMO of complex **13j** at BP86/TZ2P$^+$ (energy cut-offs of MO plots 0.033).

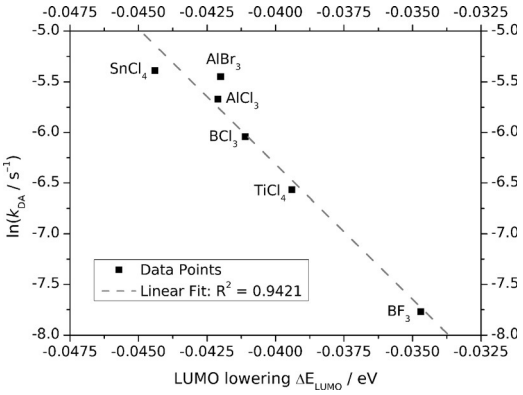

Figure 7. Plot of the LUMO shifts ΔE_{LUMO} (M06-2X/def2-TZVP) of **10** upon formation of adducts **13** versus the $\ln(k_{DA})$ of the Diels–Alder reaction.

strong activation of **10** by adduct **9j** in catalysis of the model Diels–Alder reaction and the calculated high ΔE_{LUMO} required a more detailed investigation.

To explain the unusual behaviour of $SnCl_4$, the optimised structures and especially the geometry of $SnCl_4$ in **9j** and **13j** were analysed more closely (Figure 8). A rather unusual change in coordination geometry of $SnCl_4$ was found when comparing $SnCl_4$–CBS adduct **9j** and **10**–$SnCl_4$–CBS adduct **13j**. In **9j**, the chlorine atoms are arranged axially resulting in a triangular bipyramidal environment for the tin atom. In **13j** the axial chlorine atom Cl4 is bent in the plane by 37.0° resulting in an equatorial conformation. Furthermore, this is accompanied by a shortening of the tin–nitrogen bond by 0.18 Å.

Only limited reports on structural aspects on the coordination of $SnCl_4$ to different Lewis bases are available.[22] A theoretical study by Frenking et al. dealt with the coordination of $SnCl_4$ to ammonia and pyridine, respectively. They exclusively observed the axial isomer for coordination of $SnCl_4$ to ammonia and for coordination to pyridine both isomers were identified as two closely spaced minima.[23] They postulated steric reasons for this effect but did not further investigate this

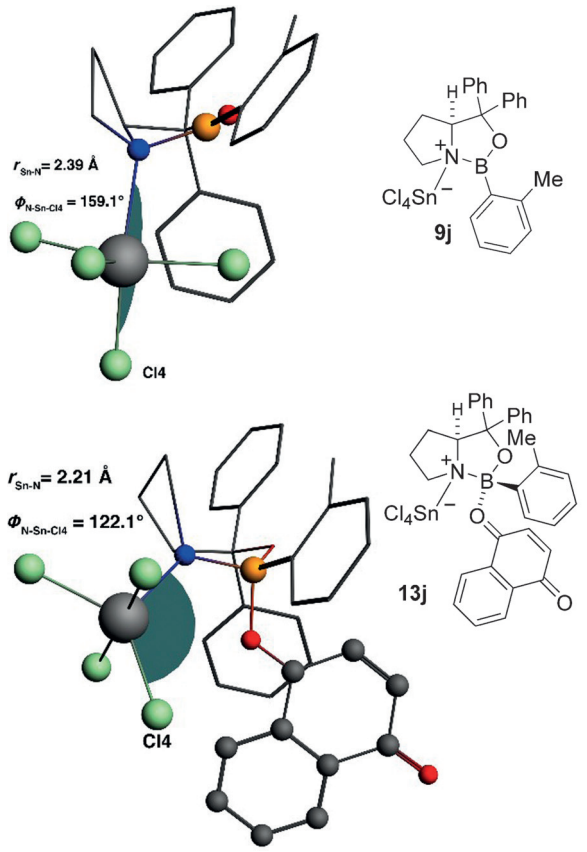

Figure 8. Optimised geometries for $SnCl_4$–CBS complex **9j** and **10**–$SnCl_4$–CBS adduct **13j** at M06-2X/def2-TZVP level, showing the change of the coordination geometry at the tin atom from **9j** to **13j** upon coordination of **10**.

aspect. Experimental insights in coordination geometries are even rarer. To the best of our knowledge, there is only one crystal structure of a classical Lewis acid base adduct present in literature where $SnCl_4$ adopted an axial conformation upon coordination to quinuclidine.[24]

Quantum chemical calculations: bonding analysis

In order to quantify the impact of this conformational change as well as its rationale, the bonding situation in **9** and **13** were studied in more detail. Therefore, the bond between the Lewis acids and the CBS fragment in adducts **9** and **13** were analysed using EDA-NOCV (energy decomposition analysis combined with natural orbitals for chemical valence). EDA analysis allows a partition of the bond energy ΔE_{int} (interaction energy) into its components ΔE_{Pauli} (Pauli repulsion energy), $\Delta E_{orbital}$ (orbital interaction energy) and ΔE_{elstat} (electrostatic interaction energy) and furthermore by linkage with NOCV theory a breakdown of $\Delta E_{orbital}$ in contributions of different fragment orbitals, thus allowing assessment of the proportion of different bond types.[25]

The results of the EDA calculations for **9** and **13** are shown exemplarily for $AlCl_3$, $SnCl_4$ and $TiCl_4$ in Table 3. A closer look on the energy terms gives an indication for the unusual strong activation of **10** by $SnCl_4$–CBS adduct **9j** within the 1,4-naphthoquinone complex **13j**. The interaction energy ΔE_{int} of $SnCl_4$ in the Lewis acid–CBS **9j** adduct is by 10.7 kcal mol^{-1} lower than that of $AlCl_3$–CBS adduct **9d** whereas $TiCl_4$–CBS adduct **9k** is only 4.7 kcal mol^{-1} less stable than **9d**. This is qualitatively in line with the observed $\Delta\delta(^2H)$ values. The lower bond energy ΔE_{int} in **9j** can mainly be ascribed to high Pauli repulsion ΔE_{Pauli} and lower electrostatic interaction energy ΔE_{elstat} and simultaneously nearly the same orbital interaction energy $\Delta E_{orbital}$. As $\Delta E_{orbital}$ should predominantly be responsible for Lewis acid activation of the CBS fragment, it was further analysed by NOCV theory. By this method, the electron flow induced by bond formation can be visualised and quantified. The by far most important NOCV (Figure 9a and b) term $\Delta\rho_{\sigma,1}$ could be assigned to the $\sigma(CBS \rightarrow \sigma^*_{LA-Cl})$ bond. This term is nearly identical for **9d** and **9j** with 36.0 and 35.6 kcal mol^{-1}, respectively. This can be traced back to the number of participating chlorine atoms. In both structures, just three chlorine atoms seem to engage in donor–acceptor interaction. The axially positioned fourth chlorine atom (Cl4) in the $SnCl_4$–CBS adduct **9j** does not contribute to donor–acceptor interaction and does not show any electron-density change (Figure 9b). Accordingly, this complex geometry leads to a similar orbital interaction as in the $AlCl_3$–CBS adduct **9d**. Even if this conformation does not allow efficient interaction with the Lewis base, it seems to be sterically favoured due to a lower necessary preparation energy $\Delta E_{prep}(SnCl_4)$ of 20.7 kcal mol^{-1} for the axial conformation compared to 38.8 kcal mol^{-1} (entry **9j fixed** in Table 3, see discussion below) necessary for the equatorial conformation.

Furthermore, it allows direct stabilising interaction of the tin atom with one of the phenyl rings of the CBS backbone contributing to $\Delta E_{orbital}$ with 3.9 kcal mol^{-1}. This situation changes dramatically when 1,4-naphthoquinone (**10**) coordinates to $SnCl_4$–CBS adduct **9j** resulting in **13j**. The fourth chlorine atom changes from an axial to an equatorial conformation. EDA calculation of **13j** now show an interaction energy ΔE_{int} similar to **13d** due to a disproportional increase in orbital (−56.6 to −88.4 kcal mol^{-1}) and electrostatic interaction. The increase of the orbital term can be attributed by NOCV calculation to the conformational change and a concomitant participation of the now equatorial chlorine atom (Cl4) in donor–acceptor interaction. The most important interaction $\Delta\rho_{\sigma,1}$ with −58.8 kcal mol^{-1} is shown in Figure 9d, which is the $\sigma(HOMO_{10-CBS} \rightarrow \sigma^*_{Sn-Cl})$ bond, and it clearly verifies a participation of all four chlorine atoms. In addition, the enhanced orbital interaction seems to lead to a by 0.18 Å contracted tin–nitrogen bond, which in turn leads to a stronger electrostatic interaction. As a consequence of the change from axial to equatorial conformation seems to be clear, the question for the cause of the change arises. Especially since a comparable increase in orbital interaction could not be verified for the $TiCl_4$ adducts **13d** and **13k**.

In order to analyse the conformational change in more detail, an EDA-NOCV calculation of the $SnCl_4$–CBS adduct **9j fixed** (**9j** in the geometry of the corresponding **10**–CBS–$SnCl_4$ complex **13j**) was carried out to determine the impact of the conformational change without taking interactions with **10** into account. As shown in Table 3, the distortion of **9j** into **9j**

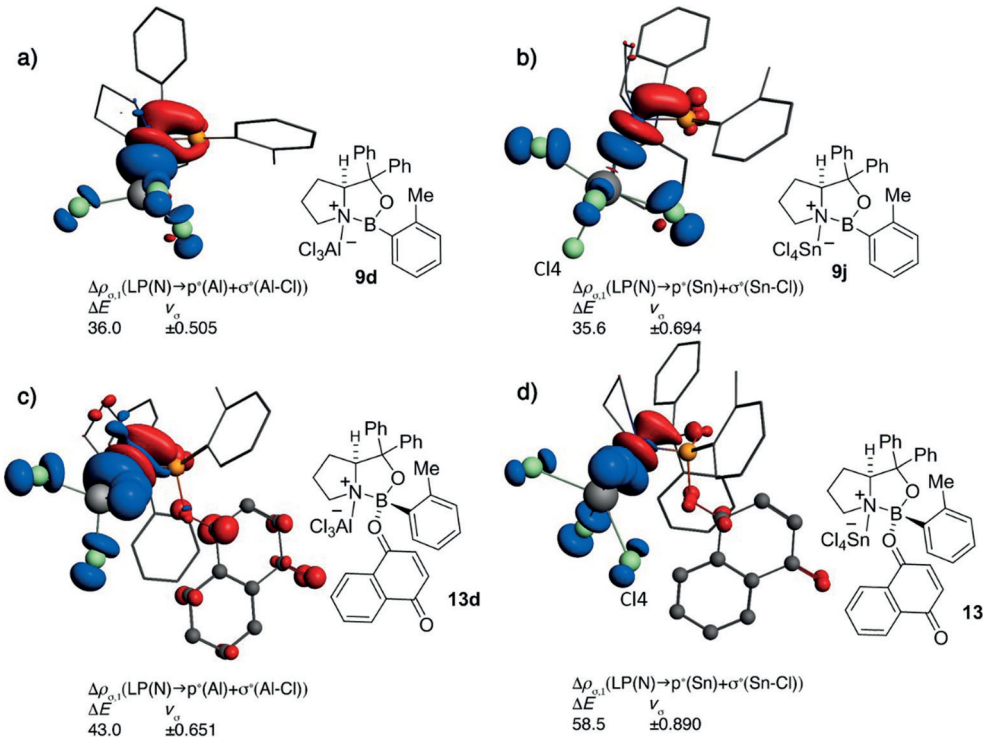

Figure 9. Plots of the NOCVs with the highest eigenvalue ($\Delta\rho_{\sigma,1}$) representing the donor–acceptor interaction (LP(N_{CBS})→LP*(Al/Sn)+σ*(LA-Cl)) in: a) **9d**, b) **9j**, c) **13d**, and d) **13j** at BP86/TZ2P^{+}. b) The missing participation of the fourth chlorine atom of $SnCl_4$ in the CBS–$SnCl_4$ bond in **9j** can be seen. d) The deformation-induced participation of this atom in the **10**–CBS–$SnCl_4$ bond upon coordination of **10** to **9j** is visible. Colour coding: red = decrease of electron density; blue = increase of electron density.

Table 3. Overview of the energy terms given by bonding analysis (EDA-NOCV) of complexes **9e**, **9j**, and **9k**, as well as adducts **13e**, **13j**, and **13k**.

Lewis acid	$AlCl_3$		$SnCl_4$			$TiCl_4$	
energy contributions	complex **9d** [kcal mol^{-1}]	adduct **13d** [kcal mol^{-1}]	complex **9j** [kcal mol^{-1}]	**9j fixed** [kcal mol^{-1}]	adduct **13j** [kcal mol^{-1}]	complex **9k** [kcal mol^{-1}]	adduct **13k** [kcal mol^{-1}]
ΔE_{int} [a]	−60.3	−79.8	−49.6	−62.0 (25.0)[e]	−80.4 (30.0)[f]	−55.6	−65.2
ΔE_{Pauli}	104.2	116.9	111.5	140.2 (25.7)[e]	148.8 (6.1)[f]	106.0	109.3
ΔE_{elstat}	−87.5	−102.7	−77.2	−106.4 (37.8)[e]	−112.8 (6.0)[f]	−83.6	−79.1
$\Delta E_{orbital}$	−58.0	−72.7	−56.6	−74.3 (31.3)[e]	−88.4 (19.0)[f]	−54.1	−67.1
ΔE_{Disp}	−19.0	−21.3	−27.3	−21.5 (−21.2)[e]	−28.0 (30.2)[f]	−23.9	−28.3
ΔE_{prep}	18.4	23.9	27.2	74.7 (174.6)[e]	44.5	39.2	39.0
$\Delta E_{prep(LA)}$ [b]	10.3	17.1	20.7	38.8 (87.4)[e]	38.8	28.0	33.4
ΔE_{bond} ($-D_e$)[c]	−41.9	−56.0	−22.5	12.7 (−156.7)[e]	−35.9 (135.4)[f]	−16.4	−26.2
$E_{HOMO(CBS)}$ [d]	−0.283	−0.254	−0.290	−0.280 (3.4)[e]	−0.251 (11.8)[f]	−0.282	−0.253

[a] $\Delta E_{int} = \Delta E_{Pauli} + \Delta E_{elstat} + \Delta E_{orb} + \Delta E_{Disp}$. [b] Contribution of the preparation energy from the LA fragment to ΔE_{prep}. [c] $\Delta E_{bond} = \Delta E_{int} + \Delta E_{prep}$. [d] Energy of the HOMO of the respective CBS fragment [eV] at M06-2X/def2-TZVP. [e] Change [%] from **9j** to **9j fixed**. [f] Change [%] from **9j fixed** to **13j**.

fixed has two important impacts on interaction energies. First, the attractive interaction energies ΔE_{elstat} and ΔE_{orb} are amplified. In particular orbital interaction is increased to −74.3 kcal mol^{-1} (+31%) due to participation of all four chlorine atoms in donor–acceptor interaction, which is in line with the results for **13j**. Even if the Pauli repulsion is increased by 28.7 kcal mol^{-1}, ΔE_{int} is 12.4 kcal mol^{-1} (25.0%) higher in energy than in the relaxed structure of **9j**. However, the increase in ΔE_{int} is overcompensated by a disproportional increase of the preparation energy ΔE_{prep} by 175% resulting in a bonding energy ΔE_{bond} of +12.7 kcal mol^{-1}. This means that although the attractive interaction in **9j fixed** is somewhat higher than in **9j**, high ΔE_{prep} and an increase in ΔE_{Pauli} makes this conformation unstable, forcing $SnCl_4$ to adopt a trigonal bipyramidal conformation **9j**.

Only after introduction of naphthoquinone, the equatorial conformation becomes thermodynamically stable mainly due to an increase of orbital interaction by 19%. The increase in ΔE_{orb} can be assigned to the enhancement of Lewis basicity of the CBS fragment **1b** upon coordination of **10** which can be seen in the increase of $\Delta E_{HOMO(10\text{–}CBS)}$ by 12% after coordination of **13**.

Apparently, the increase in Lewis basicity of the **10**–CBS fragment leads to exceeding a threshold, which only allows efficient interaction of all four chlorine atoms of $SnCl_4$ with the CBS fragment. In complex **13j** (Figure 9d) the distortion of the complex geometry leads to an enhanced Lewis acidity where all four chlorine atoms show participation in electron density delocalisation. This results in an increased Lewis acidity of $SnCl_4$ in **13j** compared to **9j**, which can be observed in a high k_{DA} value making $SnCl_4$ in the equatorial conformation a similar potent Lewis acid as $AlBr_3$.

Although the threshold in Lewis basicity for efficient interaction is the main factor that influences the interplay between both conformations, a second interaction that pushes **13j** towards the equatorial conformation could be found by analysing the NOCV interactions in **13j**. An C–H···Cl interaction $\Delta\rho_{\sigma,6}$ between the hydrogen atom of **10** at position 5 with the chlorine atom Cl3 could be found, which contributes about -1.9 kcal mol^{-1} (Figure 10). This further stabilizes the equatorial conformation and might be a reason for the high enantioselectivity of **9j** in the model Diels–Alder reaction. A similar halogen–hydrogen bond has been found by Fujimoto in his detailed theoretical study on $AlBr_3$–CBS adduct **9e** in the reaction of methacrolein with cyclopentadiene.[16]

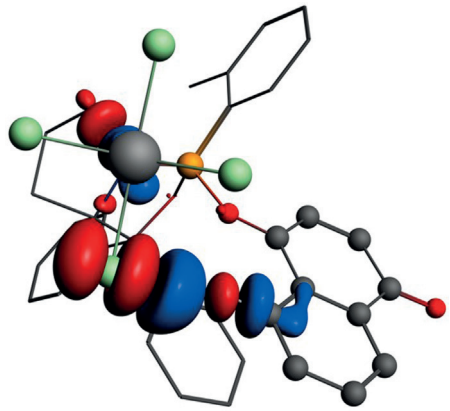

Figure 10. Plot of the NOCV interaction $\Delta\rho_{\sigma,6}$ between the $SnCl_4$ chlorine atoms and the hydrogen atom at position 5 of **10** in adduct **13j** with fragments **10**–CBS and $SnCl_4$ at BP86/TZ2P$^+$.

Conclusions

In conclusion, by combining ^{2}H NMR spectroscopic studies with in situ-IR kinetic measurements, we could demonstrate that several Lewis acids are able to activate CBS catalyst **1b** adequately for Diels–Alder reactions. This suggests the use of less aggressive acids than the commonly employed $AlBr_3$ or $HNTf_2$. The low experimentally quantified activation $\Delta\delta(^2H)$ of **1b** but large catalytic activity of $SnCl_4$–CBS adduct **9j** could be attributed to a conformational change of the chlorine atoms of $SnCl_4$ upon coordination of 1,4-naphthoquinone (**10**). This leads to a massively enhanced Lewis acidity of $SnCl_4$ within the **10**–$SnCl_4$–CBS complex **13j** and thereby to a higher activation of **10** in the Diels–Alder reaction. This behaviour could only be observed for $SnCl_4$. Trivalent Lewis acids such as $AlCl_3$, but also the tetravalent Lewis acid $TiCl_4$ did not show such a behaviour as they adopted only trigonal pyramidal or in case of $TiCl_4$ quadratic pyramidal conformation. The conformational change could be attributed to a more efficient Lewis acid base interaction upon complexation of 1,4-naphthoquinone (**10**) by raising the electron density within the CBS fragment and thus allowing an efficient donor–acceptor interaction of all four chlorine atoms of $SnCl_4$, which overcompensates the high necessary preparation energy. Furthermore, interactions of the hydrogen-atom in position 5 of the naphthoquinone with one of the chlorine atoms could be found which further stabilises the equatorial conformation.

The dependency of the acidity of group 13 based Lewis acids on their structure has been known for some time,[26] and has inspired the design of pre-organised tetrahedral group 13 Lewis acids.[27] A similar behaviour for group 4 and 14 Lewis acids has only been briefly touched on.[23] Through the presented study, both experimental and theoretical results could unravel the impact of the structural change of $SnCl_4$ on its acidity. Similar to the group-13-based Lewis acids, the design of sterically fixed tin-based Lewis acids should therefore lead to the development of novel, highly reactive catalysts.

Experimental Section

Procedure for the preparation of Lewis acid adducts [D$_1$]9 of [D$_1$]1b with stoichiometric amounts of Lewis acid

Inside a glovebox, deuterated CBS-catalyst ([D$_1$]**1b**, 32 mg, 90 μmol, 1.0 equiv) was weighed in a vial, equipped with a magnetic stirring bar. The vial was sealed with a rubber septum, transferred out of the glovebox and connected to a Schlenk line. Then CH_2Cl_2 (0.61 mL) was added, and the solution cooled to below -70 °C. A solution of the respective Lewis acid in CH_2Cl_2 (1.0 M, 90 μL, 90 μmol, 1.0 equiv) and 1 μL of $CDCl_3$ were added under constant stirring. After 15 min an aliquot of the solution (0.50 mL, 64 μmol adduct [D$_1$]**9**) was transferred into a below -70 °C precooled NMR tube, which was sealed with a rubber/PTFE septum. The sample was kept below -70 °C and analysed by NMR spectroscopy at the desired temperature.

Exemplary procedure for the ReactIR kinetic analysis of the Diels–Alder reaction of 10 with 11 by using catalysts of type 9

A 25 mL two-neck Schlenk flask was equipped with a magnetic stirring bar and the ReactIR probe head, and was connected to a Schlenk line. Under argon atmosphere, the flask was cooled to -40 °C and CH_2Cl_2 (3.0 mL), an aliquot of stock solution of **10** (4.0 mL, 0.50 mmol, 1.0 equiv, CH_2Cl_2 ($c = 125$ mmol L^{-1})), as well as isoprene (**11**, 500 μL, 4.99 mmol, 10.0 equiv) were added. Depending on the amount of catalyst solution added later, CH_2Cl_2 (0.1 or 0.4 mL) was added. The in situ FTIR spectroscopic measurement was started, as soon as there were at least 3.0 mL solution in the flask. When the temperature ($-40(\pm 1)$ °C) as well as the intensity of the IR carbonyl band of dienophile **10** at 1670 cm^{-1} were stable, an aliquot of the respective adduct **9** in CH_2Cl_2 (0.02 mmol, 4.0 mol% active complex, preparation see below) was added under vigorous stirring (final concentrations: c(**10**) = 61.7 mmol L^{-1}, c(**11**) = 617 mmol L^{-1}, c(**9**) = 2.5 mmol L^{-1}, total volume: 8.1 mL).

After 1 min the stirring speed was slightly reduced and the reaction progress was monitored until no further increase of the intensity of the IR carbonyl band of product **12** at 1696 cm^{-1} was observed. To confirm full conversion, a sample (max. 50 µL) was taken, eluted over a small pad of silica gel with *tert*-butyl methyl ether, and subjected to GC-MS analysis. The reaction was stopped by addition of saturated aqueous $NaHCO_3$ solution (4.0 mL) and stirred at room temperature for 15 min. The phases were separated and the aqueous phase was extracted with CH_2Cl_2 (4×10 mL). The combined organic phases were dried over $MgSO_4$, the solvent was removed under reduced pressure, and the raw product was stored at −20 °C under inert atmosphere until HPLC analysis. The enantiomeric ratio of the raw product was determined by HPLC analysis (Agilent Technologies 1200 Series, Chiralpak IA column, 4.6 mm× 250 mmL, 20 °C, *n*-hexane/isopropanol 99:1, flow rate: 1.0 mL min^{-1}, $\lambda = 254$ nm, $t_R = 16.0$ min (major), $t_R = 17.8$ min (minor)).

Preparation of the Lewis acid–CBS adduct solution

Inside a glove box, CBS-catalyst (**1b**; 28–30 mg, 79–85 µmol) was weighed in a vial equipped with a magnetic stirring bar. The vial was sealed with a rubber septum, transferred out of the glovebox and connected to a Schlenk line. CH_2Cl_2 (0.54 mL) was added, the solution was cooled to below −30 °C, and a solution of the respective Lewis acid in CH_2Cl_2 (1.0 m, 60 µL, 60 µmol) was added under stirring. The solution was cooled to about −50 °C and was ready for use after 10 min.

Computational details

Unconstrained structural optimisation was carried out using Gaussian 09 in version C.01.[28] Pre-optimisations were carried out using the B1B95[29] functional with the def2-SVP[30] basis set. For each structure several possible conformers were tested but only the lowest energy conformer was used for further optimisation. Refined structures were obtained by optimisation using the M06–2X[31] functional and the def2-TZVP[30] basis set with an ultra fine integration grid. This choice of computational level was motivated by previous studies of Fujimoto et al. for the CBS-catalyst.[16] Character of a stationary point was identified by subsequent frequency calculation (number of imaginary frequencies (NIMAG): 0 for minimum structures). Formation enthalpies (ΔH) including zero-point vibrational energy (ZPVE) and thermal corrections were obtained from theses frequency calculation with $T = 298.15$ K and $P = 1$ atm. HOMO/LUMO energies are given as $\Delta E_{HOMO}/\Delta E_{LUMO}$ with respect to the HOMO/LUMO energy of free CBS/naphthoquinone molecules. EDA-NOCV analysis was carried out with the ADF program version 2014.10[32] on the BP86[33]/TZ2P+[34] level using the empirical dispersion correction scheme DFT-D3.[35] All fragments were used in their singlet ground states.

Acknowledgements

We thank the Deutsche Forschungsgemeinschaft for financial support and we thank Prof. G. Frenking and L. Vondung for helpful discussions. We thank Prof. E. Meggers and Prof. P. von Zezschwitz for providing their equipment to determine enantioselectivities, as well as T. Mietke (Meggers group) and C. Pfaff (von Zezschwitz group) for their assistance.

Keywords: ab initio calculations · CBS catalyst · Diels–Alder reactions · frontier molecular orbitals · kinetics

[1] a) S. Itsuno, K. Ito, A. Hirao, S. Nakahama, *J. Chem. Soc. Chem. Commun.* **1983**, 469–470; b) S. Itsuno, K. Ito, A. Hirao, S. Nakahama, *J. Org. Chem.* **1984**, *49*, 555–557.
[2] a) E. J. Corey, R. K. Bakshi, S. Shibata, *J. Am. Chem. Soc.* **1987**, *109*, 5551–5553; b) E. J. Corey, R. K. Bakshi, S. Shibata, C.-P. Chen, V. K. Singh, *J. Am. Chem. Soc.* **1987**, *109*, 7925–7926.
[3] E. J. Corey, C. J. Helal, *Angew. Chem. Int. Ed.* **1998**, *37*, 1986–2012; *Angew. Chem.* **1998**, *110*, 2092–2118.
[4] a) E. J. Corey, T. Shibata, T. W. Lee, *J. Am. Chem. Soc.* **2002**, *124*, 3808–3809; b) D. H. Ryu, T. W. Lee, E. J. Corey, *J. Am. Chem. Soc.* **2002**, *124*, 9992–9993; c) D. H. Ryu, E. J. Corey, *J. Am. Chem. Soc.* **2003**, *125*, 6388–6390.
[5] E. J. Corey, *Angew. Chem. Int. Ed.* **2009**, *48*, 2100–2117; *Angew. Chem.* **2009**, *121*, 2134–2151.
[6] K. Futatsugi, H. Yamamoto, *Angew. Chem. Int. Ed.* **2005**, *44*, 1484–1487; *Angew. Chem.* **2005**, *117*, 1508–1511.
[7] D. Liu, E. Canales, E. J. Corey, *J. Am. Chem. Soc.* **2007**, *129*, 1498–1499.
[8] K. Mahender Reddy, E. Bhimireddy, B. Thirupathi, S. Breitler, S. Yu, E. J. Corey, *J. Am. Chem. Soc.* **2016**, *138*, 2443–2453.
[9] a) G. Zhou, Q.-Y. Hu, E. J. Corey, *Org. Lett.* **2003**, *5*, 3979–3982; b) Q.-Y. Hu, G. Zhou, E. J. Corey, *J. Am. Chem. Soc.* **2004**, *126*, 13708–13713; c) Q.-Y. Hu, P. D. Rege, E. J. Corey, *J. Am. Chem. Soc.* **2004**, *126*, 5984–5986; d) S. A. Snyder, E. J. Corey, *J. Am. Chem. Soc.* **2006**, *128*, 740–742; e) S. Hong, E. J. Corey, *J. Am. Chem. Soc.* **2006**, *128*, 1346–1352; f) J. Y. Sim, G.-S. Hwang, H. K. Kim, E. M. Ko, D. H. Ryu, *Chem. Commun.* **2007**, 5064–5064; g) S. Mukherjee, A. P. Scopton, E. J. Corey, *Org. Lett.* **2010**, *12*, 1836–1838; h) B. K. Senapati, L. Gao, S. I. Lee, G. S. Hwang, D. J. Ryu, *Org. Lett.* **2010**, *12*, 5088–5091; i) M. Y. Jin, G.-S. Hwang, H. I. Chae, S. H. Jung, D. H. Ryu, *Bull. Korean Chem. Soc.* **2010**, *31*, 727–730; j) D. R. Hookins, A. R. Burns, R. J. K. Taylor, *Eur. J. Org. Chem.* **2011**, 451–454.
[10] a) E. J. Hicken, E. J. Corey, *Org. Lett.* **2008**, *10*, 1135–1138; b) S. Jones, D. Valette, *Org. Lett.* **2009**, *11*, 5358–5361; c) M. Schubert, P. Metz, *Angew. Chem. Int. Ed.* **2011**, *50*, 2954–2956; *Angew. Chem.* **2011**, *123*, 3011–3013.
[11] a) G. Hilt, F. Pünner, J. Möbus, V. Naseri, M. A. Bohn, *Eur. J. Org. Chem.* **2011**, 5962–5966; b) G. Hilt, A. R. Nödling, *Eur. J. Org. Chem.* **2011**, 7071–7075; c) A. R. Nödling, K. Müther, V. H. G. Rohde, G. Hilt, M. Oestreich, *Organometallics* **2014**, *33*, 302–308; d) A. R. Nödling, G. Jakab, P. R. Schreiner, G. Hilt, *Eur. J. Org. Chem.* **2014**, 6394–6398.
[12] C. Sparr, E.-M. Tanzer, J. Bachmann, R. Gilmour, *Synthesis* **2010**, 1394–1397.
[13] J. N. Payette, H. Yamamoto, *Angew. Chem. Int. Ed.* **2009**, *48*, 8060–8062; *Angew. Chem.* **2009**, *121*, 8204–8206.
[14] a) R. F. Childs, D. L. Mulholland, A. Nixon, *Can. J. Chem.* **1982**, *60*, 801–808; b) M. A. Beckett, D. S. Brassington, S. J. Coles, M. B. Hursthouse, *Inorg. Chem. Commun.* **2000**, *3*, 530–533; c) L. O. Müller, D. Himmel, J. Stauffer, G. Steinfeld, J. Slattery, G. Santiso-Quiñones, V. Brecht, I. Krossing, *Angew. Chem. Int. Ed.* **2008**, *47*, 7659–7663; *Angew. Chem.* **2008**, *120*, 7772–7776; d) H. Böhrer, N. Trapp, D. Himmel, M. Schleep, I. Krossing, *Dalton Trans.* **2015**, *44*, 7489–7499.
[15] The formation of multiple species is known from Corey's reports on Brønsted acid adduct **3a** (see ref. [4c]), but in this case different ion pair species are formed.
[16] K. Sakata, H. Fujimoto, *J. Org. Chem.* **2013**, *78*, 3095–3103.
[17] M. N. Paddon-Row, L. C. H. Kwan, A. C. Willis, M. S. Sherburn, *Angew. Chem. Int. Ed.* **2008**, *47*, 7013–7017; *Angew. Chem.* **2008**, *120*, 7121–7125.
[18] Preliminary proof-of-principle studies of **9j** as catalyst in further Diels–Alder reactions showed performances of **9j** comparable to **9e**, see the Supporting Information for further details.
[19] a) R. B. Woodward, R. Hoffmann, in *The Conservation of Orbital Symmetry*, Verlag Chemie, Weinheim, **1970**; b) J. Sauer, R. Sustmann, *Angew. Chem. Int. Ed. Engl.* **1980**, *19*, 779–807; *Angew. Chem.* **1980**, *92*, 773–801; c) O. F. Guner, R. M. Ottenbrite, D. D. Shillady, P. V. Alston, *J. Org. Chem.* **1987**, *52*, 391–394.

[20] a) P. Laszlo, M. Teston, *J. Am. Chem. Soc.* **1990**, *112*, 8750 – 8754; b) P. Laszlo, M. Teston, *Tetrahedron Lett.* **1991**, *32*, 3837 – 3838.
[21] Coordination of indium-based Lewis acids to the CBS-fragment was confirmed by analysis of the crucial bond lengths and by EDA-NOCV calculation.
[22] E. I. Davydova, T. N. Sevastianova, A. V. Suvorov, A. Y. Timoshkin, *Coord. Chem. Rev.* **2010**, *254*, 2031 – 2077.
[23] E. I. Davydova, A. Y. Timoshkin, T. N. Sevastianova, A. V. Suvorov, G. Frenking, *Comput. Theor. Chem.* **2006**, *767*, 103 – 111.
[24] W. A. Grigsby, T. S. Morien, C. L. Raston, B. W. Skelton, A. H. White, *Aust. J. Chem.* **2004**, *57*, 507 – 508.
[25] a) K. Kitaura, K. Morokuma, *Int. J. Quantum Chem.* **1976**, *10*, 325 – 340; b) T. Ziegler, A. Rauk, *Theor. Chim. Acta* **1977**, *46*, 1 – 10; c) M. Mitoraj, A. Michalak, *J. Mol. Model.* **2008**, *14*, 681 – 687; d) A. Michalak, M. Mitoraj, T. Ziegler, *J. Phys. Chem. A* **2008**, *112*, 1933 – 1939; e) M. Mitoraj, A. Michalak, T. Ziegler, *J. Chem. Theory Comput.* **2009**, *5*, 962 – 975; f) M. Mitoraj, A. Michalak, T. Ziegler, *Organometallics* **2009**, *28*, 3727 – 3733; g) M. Srebro, A. Michalak, *Inorg. Chem.* **2009**, *48*, 5361 – 5369; h) I. Purushothaman, S. De, P. Parameswaran, *RSC Adv.* **2014**, *4*, 60421 – 60428.
[26] a) C. Loschen, K. Voigt, J. Frunzke, A. Diefenbach, M. Diedenhofen, G. Frenking, *Z. Allg. Anorg. Chem.* **2002**, *628*, 1294 – 1304; b) G. Frenking, K. Wichmann, N. Fröhlich, C. Loschen, M. Lein, J. Frunzke, V. M. Rayón, *Coord. Chem. Rev.* **2003**, *238 – 239*, 55 – 82; c) F. Bessac, G. Frenking, *Inorg. Chem.* **2006**, *45*, 6956 – 6964; d) L. A. Mück, A. Y. Timoshkin, M. von Hopffgarten, G. Frenking, *J. Am. Chem. Soc.* **2009**, *131*, 3942 – 3949; e) A. S. Lisovenko, A. Y. Timoshkin, *Inorg. Chem.* **2010**, *49*, 10357 – 10369; f) L. A. Mück, A. Y. Timoshkin, G. Frenking, *Inorg. Chem.* **2012**, *51*, 640 – 646.
[27] H. Zhu, E. Chen, *Inorg. Chem.* **2007**, *46*, 1481 – 1487.
[28] Gaussian 09, Revision C.01, M. J. Frisch, G. W. Trucks, H. B. Schlegel, G. E. Scuseria, M. A. Robb, J. R. Cheeseman, G. Scalmani, V. Barone, B. Mennucci, G. A. Petersson, H. Nakatsuji, M. Caricato, X. Li, H. P. Hratchian, A. F. Izmaylov, J. Bloino, G. Zheng, J. L. Sonnenberg, M. Hada, M. Ehara, K. Toyota, R. Fukuda, J. Hasegawa, M. Ishida, T. Nakajima, Y. Honda, O. Kitao, H. Nakai, T. Vreven, J. A. Montgomery, Jr., J. E. Peralta, F. Ogliaro, M. Bearpark, J. J. Heyd, E. Brothers, K. N. Kudin, V. N. Staroverov, R. Kobayashi, J. Normand, K. Raghavachari, A. Rendell, J. C. Burant, S. S. Iyengar, J. Tomasi, M. Cossi, N. Rega, J. M. Millam, M. Klene, J. E. Knox, J. B. Cross, V. Bakken, C. Adamo, J. Jaramillo, R. Gomperts, R. E. Stratmann, O. Yazyev, A. J. Austin, R. Cammi, C. Pomelli, J. W. Ochterski, R. L. Martin, K. Morokuma, V. G. Zakrzewski, G. A. Voth, P. Salvador, J. J. Dannenberg, S. Dapprich, A. D. Daniels, Ö. Farkas, J. B. Foresman, J. V. Ortiz, J. Cioslowski, D. J. Fox, Gaussian, Inc., Wallingford CT, **2009**.
[29] A. D. Becke, *J. Chem. Phys.* **1996**, *104*, 1040 – 1046.
[30] F. Weigend, R. Ahlrichs, *Phys. Chem. Chem. Phys.* **2005**, *7*, 3297 – 3305; b) B. Metz, H. Stoll, M. Dolg, *J. Chem. Phys.* **2000**, *113*, 2563 – 2569; c) F. Weigend, *Phys. Chem. Chem. Phys.* **2006**, *8*, 1057 – 1065.
[31] a) Y. Zhao, D. G. Truhlar, *Theor. Chem. Acc.* **2008**, *120*, 215 – 241; b) Y. Zhao, D. G. Truhlar, *Acc. Chem. Res.* **2008**, *41*, 157 – 167.
[32] a) G. te Velde, F. M. Bickelhaupt, E. J. Baerends, C. Fonseca Guerra, S. J. A. van Gisbergen, J. G. Snijders, T. Ziegler, *J. Comput. Chem.* **2001**, *22*, 931 – 967; b) C. Fonseca Guerra, J. G. Snijders, G. te Velde, E. J. Baerends, *Theor. Chem. Acc.* **1998**, *99*, 391 – 403; c) ADF2014, SCM, Theoretical Chemistry, Vrije Universiteit, Amsterdam, The Netherlands: http://www.scm.com.
[33] a) J. Perdew, *Phys. Rev. B* **1986**, *33*, 8822 – 8824; b) A. Becke, *Phys. Rev. A* **1988**, *38*, 3098 – 3100.
[34] E. van Lenthe, E. J. Baerends, *J. Comput. Chem.* **2003**, *24*, 1142 – 1156.
[35] a) S. Grimme, J. Antony, S. Ehrlich, H. Krieg, *J. Chem. Phys.* **2010**, *132*, 154104; b) S. Grimme, S. Ehrlich, L. Goerigk, *J. Comput. Chem.* **2011**, *32*, 1456 – 1465.

Received: May 19, 2016
Published online on August 5, 2016